Effect of Plasma Treatments on Wettability of Polysulfone and Polyetherimide

K. ASFARDJANI,[1] Y. SEGUI,[1,]* Y. AURELLE,[2] and N. ABIDINE[3]

[1]Laboratoire de Génie Electrique, Université Paul Sabatier, 31062 Toulouse, Cedex, France,
[2]Laboratoire de Chimie et de Génie de l'Environnement, 31077 Toulouse, Cedex, France,
and [3]Lyonnaise des Eaux, Laboratoire Membranes, 31432 Toulouse, Cedex, France

SYNOPSIS

Experimental results on plasma treatments of polysulfone and polyetherimide to improve the wettability of these polymers are presented. The plasma is characterized by optical emission spectroscopy. The wettability of the polymer surfaces were checked by contact angle measurements and ESCA is used to compare the surfaces before and after plasma treatment. Correlations between contact angle, concentration of oxygen at the surface, and optical emission intensity of the OH radical have been established. Optimization of operational plasma parameters leading to the best wettability of the treated samples is reported.

INTRODUCTION

In many technical applications, the desired surface and volume properties are not the same. Hence, it becomes difficult for a single material to fit both surface and volume requirements. At least for this reason, surface treatment and surface modification of polymeric materials is a domain of growing interest. Purely chemical,[1] purely physical,[2] and combined physical and chemical[3,4] processes have been used to modify the surface of a polymer. In the last group, plasma techniques seem to be very powerful because it is a low-temperature treatment, applicable to a large variety of materials, and able to change the surface properties to a large extent (e.g., from wettability to impermeabilisation).[5] The main drawbacks of this technique are:

1. The transfer from a small experimental setup to a large reactor fitting the real size and geometry of the items considered is not a simple homothetie.
2. A good understanding of the interactions between plasma species and treated surfaces,

necessary to have a good control on the plasma parameters, is often very difficult to achieve.

This article deals with the latter aspect. It is an attempt to establish relationships between three sets of parameters: (1) macroscopic parameters of the plasma (pressure, power, geometrical parameters); (2) composition of the gas phase with particular attention to the species responsible for surface modifications; and (3) composition and properties of the surface after plasma treatments.

The first set of parameters is experimentally fixed during the plasma treatment. The plasma gas phase composition was checked by optical emission spectroscopy; the changes in surface composition were controlled by ESCA measurements. The surface wettability was evaluated by contact angle method, while the hydrophilic properties were determined by Hamilton's method.[6]

From a technological point of view, the aim of this work is to show how a plasma process has been optimized to give the best wettability of two polymers—polysulfone (PS) and polyetherimide (PEI)—which are of great interest to make ultrafiltration and microfiltration membranes. Of course, in this case, wettability is one of the most important surface properties for these polymers.

---

* To whom correspondence should be addressed.

EXPERIMENTAL

Polymers Substrates

The substrates used in this study are PS and PEI membranes. They are either plane membranes or hollow fibers. A sample of flat membrane 2 × 2 cm or a hollow fiber was introduced in the reactor after cleaning with distilled water and alcohol and drying.

The general formulae of these two polymers are given below:
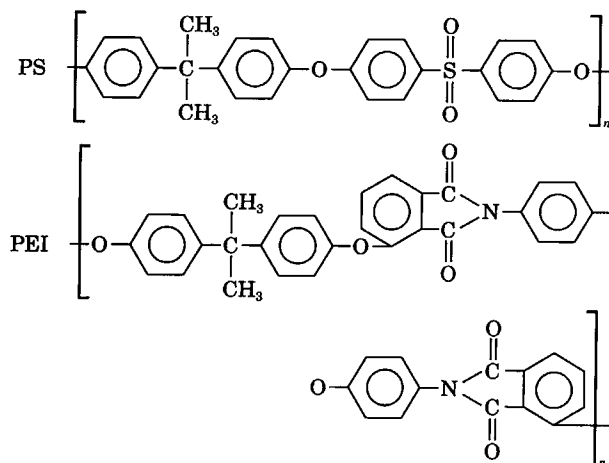
Glow Discharge

A radio frequency (13.56 MHz) glow discharge system used to create the plasma is schematically shown in Figure 1. The shape and size of the Pyrex glass reaction chamber (80 mm inner diameter and 1,000 mm long) was designed for plasma treatment of fibers.
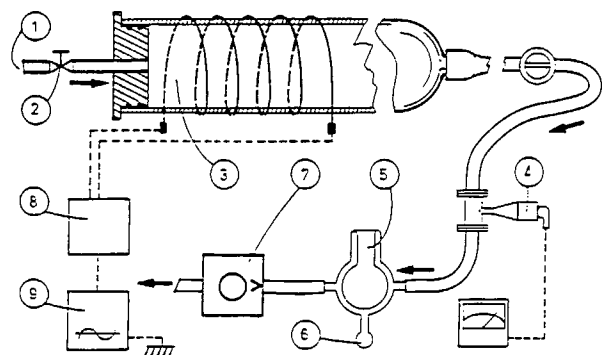

Figure 1 Experimental setup. (1), gas; (2), needle valve; (3), plasma; (4), pressure gauge; (5), nitrogen liquid; (6), trap; (7), pump; (8), matching; (9), generator frequency 13.56 MHz.

The reactor is fitted with a monomer inlet, pressure gauge, vacuum system, and a matching network between the RF power source and the inductive coil.

The parameters for the experiments are listed as below:

- operating gas pressure (P), $1 < P < 20$ Pa
- generator power (W), $10 < W < 200$ W
- distance of the sample from the center of the induction coil (d), $0 < d < 90$ cm

Besides these operational parameters, the geometry of the reactor can drastically affect the process,[7] in particular through the residence time of the species in the plasma zone as well as in the sample zone.

Two gases were used to create the plasma: H_2O and air. The reasons for this choice were their ability to generate oxygenated species and their relatively simple structures, making easier some hypothesis on chemical reactions taking place during the process.

Methods of Characterization

Wettability was assessed by two contact-angle techniques: (1) Hamilton's method and (2) conventional method using a distillated water drop.

Some other attempts for hollow fibers like:

1. measurement of lifted-up liquid weight by means of a wetting tensiometer[8]
2. measurement of a liquid meniscus height[8]
3. characterization of drop profile (the drop being located at the fiber surface)

have not been successfully used because of either the low sensitivity of the measuring apparatus (1), (2), or the geometry of the sample (3).

Figure 2 shows a schematic representation of the experimental setup used for contact angle measurements. The main interest of the video system was a very fast recording of the observed contact angle immediately after the deposition of the water drop at the surface of the sample. Then, the effects of capillarity phenomena across the polymer membrane were drastically reduced.

Figure 3 represents the wettability cell used to determine the hydrophilicity of the surfaces according to Hamilton's method. The cell was first filled with distilled water, then the sample on its sample holder was fixed inside the cell, and finally a microdrop of n-octane (2 μL) was formed inside the water at the surface of the sample. The contact angle between the drop of n-octane and the surface was
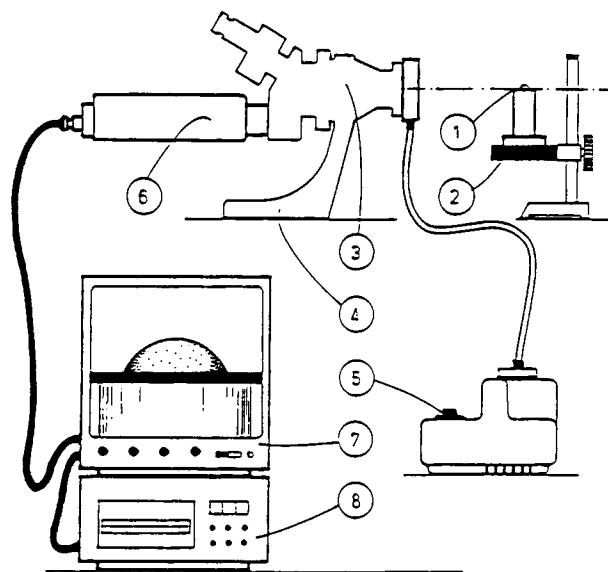
Figure 2 Experimental device for measuring contact angles. (1), sample holder; (2), support; (3), microscope; (4), mobile holder; (5), lighting system; (6), camera; (7), video screen; (8), printer.

then measured using the experimental setup shown in Figure 2.

Hamilton's method is based on the finding that the dispersion force contributions to the surface free energies of n-octane and water are equal. This enabled a simple method to characterize the hydrophilic nature of solid surfaces. This technique involves measuring octane contact angles on solid surfaces under water and calculation of interfacial energy. Nonhydrophilic solids unable to interact by polar forces exhibit a predicted 50° contact angle, whereas those able to interact by polar forces give values greater than 50°. The deviation of the contact angle from 50° interfacial stabilization energy mainly comes from the polar forces.

It must be pointed out that the water–polymer interaction surface leads to a surface reconstruction for the polymer sample due to a driving force generated by the polar nature of the water. Lavielle[9] showed that under this effect some polar groups of the polymer reorient to come to the surface. Consequently, the hydrophilicity measured under these circumstances is the maximum value exhibited by the material, provided enough time is allowed for such orientation.

The surface composition and structure was investigated by ESCA. The ESCA spectra were recorded with an Escalab MKII employing an AlK_α exciting radiation at 15 kV, 20 mA, $6.7 \cdot 10^{-8}$ Pa.

ESCA involves the measurement of binding

energies of electrons ejected from the surface region (0–50 Å) upon interaction with a monoenergetic beam of X-rays. ESCA analysis of the C_{1S} and O_{1S} regions indicates the oxidation degree and the percentage concentration of various oxygenated groups (C=O; C–O; O–H; C=O) at the surface region.

$$\begin{array}{c} | \\ O \end{array}$$

The contributions due to the various chemical groups in the C_{1s} spectra are obtained by deconvoluting the peak envelope into elementary peaks. A fitting technique involving a series of Gaussian/Lorentzian peaks at known binding energies was developed using a computer program.

In ESCA analysis, it is usual to etch the first surface layers to eliminate surface contamination; however, for polymeric materials this procedure can change the surface structure[10] and lead to erroneous interpretation. In this work, all measurements were performed without etching. Because interpretations are based on a comparison between plasma treated and nontreated samples, it is believed that the contamination layer does not much influence our conclusions.

Optical Emission Spectroscopy

Among the plasma diagnostic techniques, optical emission spectroscopy has three advantages making it very useful for our purposes. First, it is a nonperturbing technique[11]: There is no interaction between the measuring system and the plasma itself. Second, it is relatively easy to obtain a spatially resolved emission spectroscopy. Thus, it becomes possible to check the homogeneity of the plasma and, even-
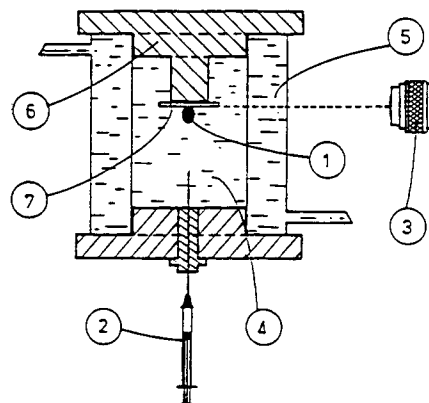

Figure 3 Sketch of the wettability cell. (1), drop of hydrocarbon; (2), syringe; (3), microscope; (4), aqueous phase; (5), thermostating double wall; (6), changeable support; (7), sample in test.
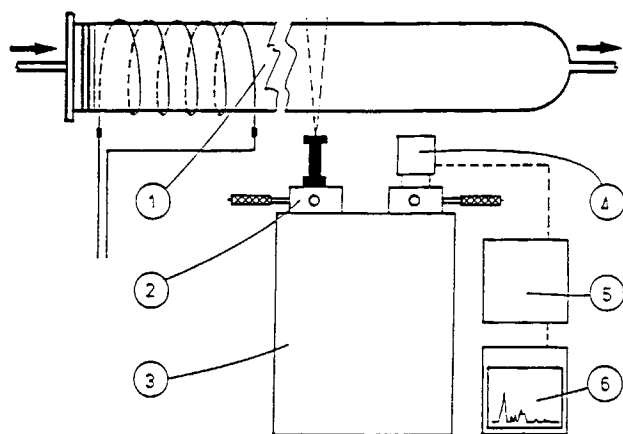
Figure 4 Optical emission spectroscopy analysis device. (1), plasma; (2), gauged slit; (3), monochromator; (4), photomultiplier; (5), microprocessor; (6), plotter.

tually, to correlate the variations of emission to the effect of plasma treatment. Finally, the emission wavelength of the oxygenated groups like OH lies in the visible or near UV range, which makes determining their measurements easy. We were particularly interested by OH emission lines (e.g., 306.3 nm) because this group is created in large quantity in H_2O plasmas. A schema of the measurement setup is given in Figure 4. A Jobin Yvon HR320 monochromator gives a wavelength resolution of 0.4 Å, enough in this case to analyse the emission lines. The wavelength allowed by a 1,200 grooves/mm grating ranges from 190–900 nm.

An Hamamatsu R92 Z photomultiplier transform the optical signal into an electrical signal measured

by a Keithley 916 picoameter. Finally, an X–Y recorder gives the optical spectra of the discharge. The spatial resolution of this experimental setup along the main axis of the reactor was estimated to be 10 mm.

RESULTS AND DISCUSSION

Influence of the Plasma Operational Parameters on the Wettability of PEI and PS

Electrical Power

Figure 5 shows the effect of the electrical power applied to the plasma on the water contact angle for PEI membranes. Several curves have been plotted for pressures ranging from 0,065–0,200 mbars (6.5–20 Pa) and samples located under the inductive coil or 15, 30, 45, and 75 cm away from the coil. In all cases, the general shape of the curve Θ vs. power is the same. Only the value of the power giving the minimum contact angle, i.e., the best wettability, changes as a function of pressure and sample position.

Pressure of the Gas Phase

Figure 6 gives an example of the effect of the pressure on the contact angle. The substrate used was PEI and the gas water vapour. An increase in the gas pressure leads at first to a decay of the contact angle, followed by an increase. Whatever the other plasma conditions (power and location of the sample), the minimum value for Θ occurs at the same value of
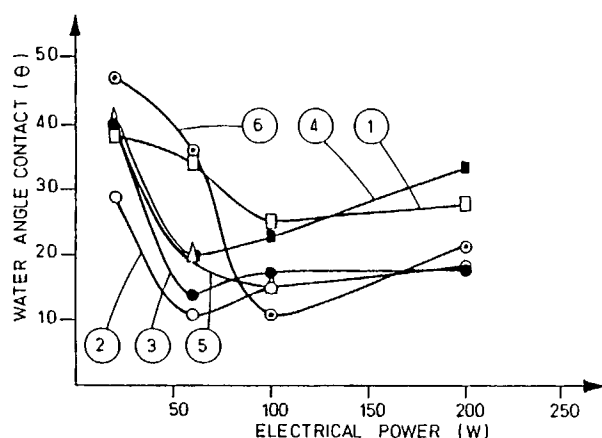

Figure 5 Effect of the electrical power on the water contact angle (PEI). (1), $P = 0.065$ mbar, $d = 15$ cm; (2), $P = 0.1$ mbar, $d = 15$ cm; (3), $P = 0.2$ mbar, $d = 15$ cm; (4), $P = 0.1$ mbar, $d = 0$ cm; (5), $P = 0.1$ mbar, $d = 30$ cm; (6), $P = 0.2$ mbar, $d = 45$ cm.

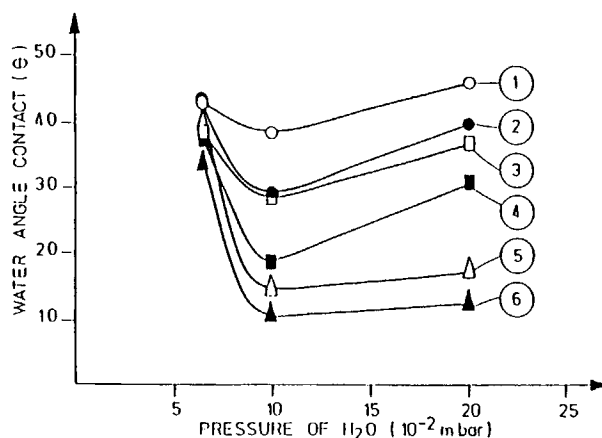**Figure 6** Effect of pressure on the water contact angle (PEI). (1), $W = 60$ W, $d = 75$ cm; (2), $W = 20$ W, $d = 15$ cm; (3), $W = 60$ W, $d = 45$ cm; (4), $W = 60$ W, $d = 30$ cm; (5), $W = 100$ W, $d = 15$ cm; (6), $W = 60$ W, $d = 15$ cm.
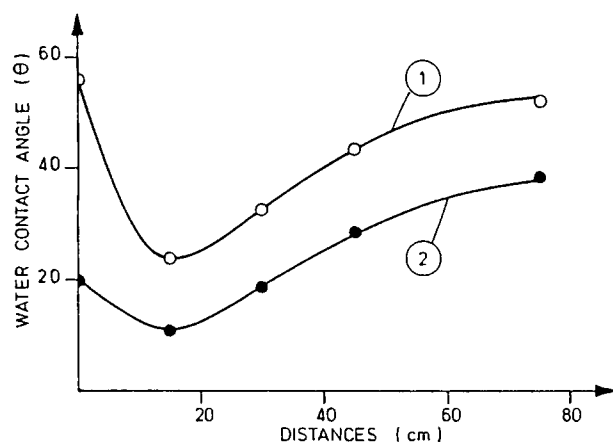
Figure 7(a)   Effect of distance on the water contact angle. (1), PS: $P = 0.1$ mbar, $W = 60$ W; (2), PEI: $P = 0.1$ mbar, $W = 60$ W.

the water pressure. However, it can be observed that at lowest power or when the sample is located far away from the coil (45 and 75 cm) the range of variation of the contact angle becomes shorter. For example, Figure 6 shows:

$\Delta\Theta = 5°$ for $W = 60$ W and $d = 75$ cm (curve 1) and

$\Delta\Theta = 13°$ for $W = 20$ W and $d = 15$ cm (curve 2),

whereas $\Delta\Theta = 25°$ for $W = 60$ W and $d = 15$ cm (curve 6).

Location of the Sample in the Reactor

The location of the sample is measured by the distance of the sample from the center of the coil ($d = 0$ when the sample is located in the middle of the coil).

Figure 7(a) shows the curves of Θ vs. distance from the coil for PEI and PS samples for the same plasma conditions. Both curves exhibit a minimum value for the contact angle Θ when the sample is located about 15 cm from the coil. Figure 7(b) shows the same dependence with other plasma parameters (power and pressure have been changed). These results have been selected to show the effect of four values of the electrical power at 0.1 mbar and the effect of three different pressures at 60 W. It is difficult to observe clear trends from these results, but this is not surprising if we consider that the dependance of Θ as a function of W or P is not linear (Figs. 5 and 6).

Interpretation

A qualitative interpretation of these experimental results can be made on the basis of two considerations:

1. In a plasma process involving polymeric materials and oxygenated species, two processes take place simultaneously[12]: (i) Etching of the surface through reactions of atomic oxygen coming from the plasma phase with carbon atoms of the substrate surface giving volatile reaction products:

$$XO^• + C \rightarrow CO_X$$
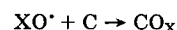
Ionic bombardment can also give the etching through physical sputtering. (ii) Deposition process by combination of species from the plasma and atoms at the surface of the sample. For example:

$$\begin{array}{ccc} CH_3 & & CH_2OH \\ | & & | \\ -C- \; + OH^• \rightarrow & -C- & + H^• \end{array}$$
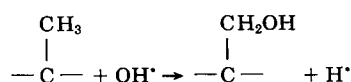
The balance between these two processes depends on the parameters of the experiment.

2. Power and pressure modify the electron energy distribution function (EEDF) in the plasma. An increase of the power and a decay of the pressure lead to an increase in the mean energy of the electrons. Moreover, this in-
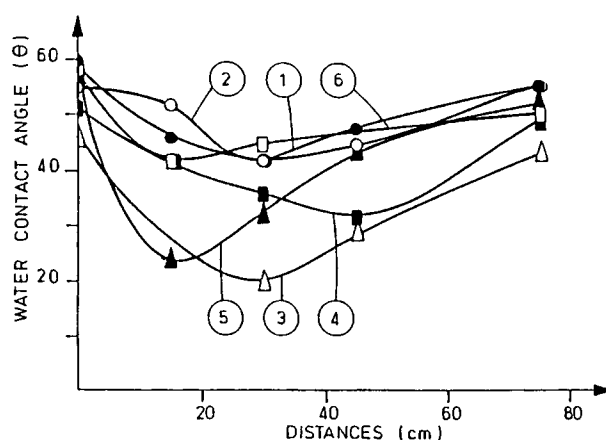

Figure 7(b)   Effect of distance on the water contact angle (PS). (1), $P = 0.2$ mbar, $W = 60$ W; (2), $P = 0.45$ mbar, $W = 60$ W; (3), $P = 0.1$ mbar, $W = 200$ W; (4), $P = 0.1$ mbar, $W = 100$ W; (5), $P = 0.1$ mbar, $W = 60$ W; (6), $P = 0.1$ mbar, $W = 20$ W.

crease in pressure leads to an increase in the number of species in the reactor.

The effect of the power (Fig. 5) can be understood by an increase of the mean energy of the electrons, which leads to an increase in the rate of formation of chemically active species through dissociation reactions like:

$$H_2O + e \rightarrow OH^{\cdot} + H^{\cdot} + e$$
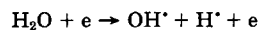
where the rate of production of OH and H radicals are related to the number of electrons energetically higher than a threshold energy for the dissociation and the cross-section for this interaction. In the ESCA section, it will be demonstrated that the grafting of oxygenated species is responsible for the increase of the wettability of the plasma-treated polymers.

Above a power threshold, the contact angle increases again because the probability of etching is higher than that of grafting. This is a well-known phenomenon already observed for many polymers interacting with oxygenated plasmas.[12] However, the detail of the etching process in this case is not yet clear: It could be due to energetic ion bombardment or to a chemical etching or ion bombardment enhanced chemical etching.

The influence of pressure (Fig. 6) can be understood by considering the two effects of pressure increase: First, the number of H_2O molecules increases, leading to an increase in the number of grafting species in the gas phase. Second, the mean free path of the electrons decreases; hence, the EEDF is moved toward lower energies according to the dissociation

reaction of H_2O indicated above, leading to a decay of the production of grafting species.

The decay of the contact angle in the first part of the curve is due to the first of these effects, whereas the increase in the second part of the curve is due to the second one. The same interpretation explains why the effect of pressure is less important at lower powers or when the sample is far away from the coil: At lower powers, the mean energy of the electrons is lower, and consequently the dissociation reactions less effective. At larger distances from the coil, the chemically active radicals created near the coil have enough time to recombine in the gas phase or at the wall of the reactor; hence, grafting also becomes less effective.

The effect of sample location with respect to the inductive coil is again the balance between etching (near the coil) and grafting. A minimum is, however, observed instead of a constant decay because there is a decay of chemically active species due to loss reactions between radicals in the gas phase or between the reactor walls and radicals.

Finally, to conclude this section, Tables I and II give the best results from the point of view of wettability and the plasma conditions used to obtain them.

Table I also gives the values of I_{SW} (interfacial stabilization energy) deduced from the Hamilton's method. I_{SW} is a quantitative evaluation of the hydrophilicity of the polymer surface. These results show the contact angle of n-octane drop is more than twice the initial value once air or water vapour plasma treatment was made. The increase of the n-octane contact angle can be related quantitatively to the magnitude of the solid's polar interactions. I_{SW} originating from nondispersive (polar) forces

Table I   Correlations Between Plasma Treatment–Operative Conditions and Hydrophibility of Solids (Hamilton's Method)

Polymer Type	Plasma Treatment Operative Conditions				Contact Angle n-octane/ water/solid	Interfacial Stabilization Energy from Polar Forces I_{SW} (ergs/cm)
	Nature	W (watts)	P (mbar)	d (cm)		
PS	Untreated				68°	11.5
PS	Air	300	$5 \cdot 10^{-2}$	44	144.5°	67
PS	Air	50	$5 \cdot 10^{-2}$	13	133°	63
PS	Air	50	$3 \cdot 10^{-2}$	35	124°	57
PS	Water	50	$1 \cdot 10^{-2}$	36	153°	73
PS	Water	50	$1 \cdot 10^{-2}$	54	151°	72
6.6. Nylon	Untreated				140°*	71*
					Hamilton Values (5)	

* Surface tensions and interfacial tension are different from our values.

Table II   Correlations Between Plasma Treatment—Operative Conditions and Wettability of Treated Polymer Surface
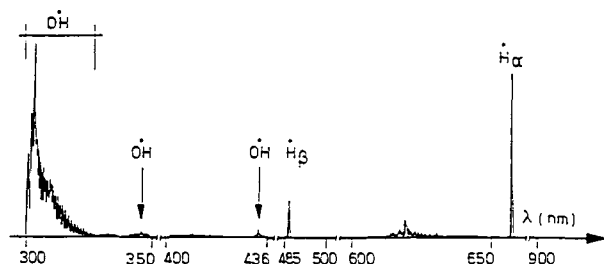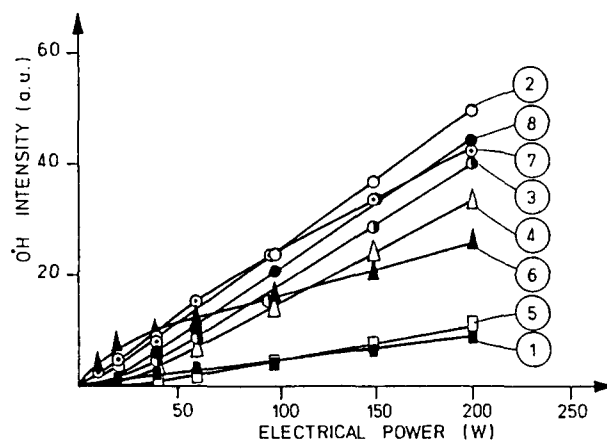
Polymer Type	Plasma Treatment Operative Conditions			Contact Angle Water/ Air/Solid
	W (watts)	P (mbar)	d (cm)	
PEI	Untreated			68°
PEI	200	0.065	45	16–18°
PEI	100	0.2	45	10–11°
PEI	100	0.2	30	11–13°
PEI	60	0.2	15	13–15°
PEI	100	0.1	30	15°
PEI	200	0.1	45	12–14°
PS	Untreated			75°
PS	60	0.1	15	23–25°
PS	200	0.1	30	20°
PS	100	0.2	15	25–26°
PS	200	0.2	45	15°

Figure 9   Effect of electrical power on OH intensity. (1), $P = 0.1$ mbar, $d = 0$ cm; (2), $P = 0.1$ mbar, $d = 15$ cm; (3), $P = 0.1$ mbar, $d = 30$ cm; (4), $P = 0.1$ mbar, $d = 45$ cm; (5), $P = 0.1$ mbar, $d = 75$ cm; (6), $P = 0.045$ mbar, $d = 15$ cm; (7), $P = 0.065$ mbar, $d = 15$ cm; (8), $P = 0.2$ mbar, $d = 15$ cm.

calculated from contact angle values is six times greater for plasma-treated samples than for untreated ones. They are very close to those determined for nylon 6-6 by Hamilton ($\Theta = 140°$, $I_{SW} = 71$ ergs/cm^2).

Correlations Between Optical Emission Spectroscopy of the Plasma and Wettability of Treated Polymer Surfaces

In the discussion of the previous section, oxygenated radicals have been involved several times. In this section, optical spectroscopy of the plasma gives some evidence of these radicals. Also, their effect on the wettability of the polymer surface is experimentally demonstrated.

A general survey of the optical emission spectra of an H_2O plasma between 300 and 900 nm is given in Figure 8. A detailed analysis of the spectra is not

the purpose of this article. We want to emphasize the fact that the main peaks are due to OH and H radicals. In the following, we concentrate on the OH emission peak at 307.6 nm.

The intensity of a given species A is given by[13]:

$$I_A = n_e n_A \int f(E) \sigma_{A^* \to A}(E) EdE, \qquad (1)$$

where n_e and n_A are the electron density and the density of species A at the ground state, $f(E)$ is the

Figure 8   Optical emission spectra of H_2O plasma. P, 0.1 mbar; W, 100 W; d, 15 cm.
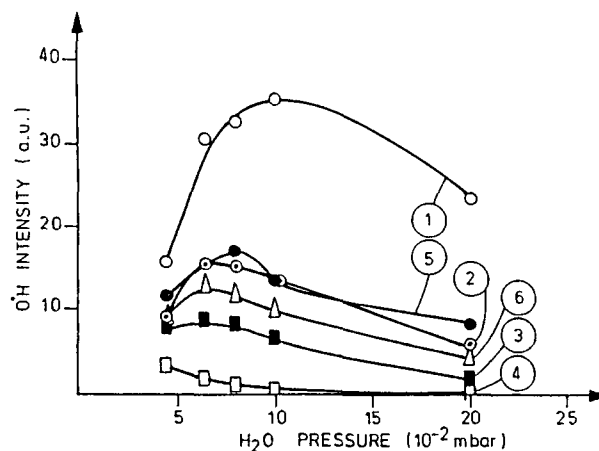
Figure 10   Effect of H_2O pressure on OH intensity. (1), $W = 20$ W, $d = 45$ cm; (2), $W = 100$ W, $d = 45$ cm; (3), $W = 60$ W, $d = 45$ cm; (4), $W = 200$ W, $d = 45$ cm; (5), $W = 60$ W, $d = 15$ cm; (6), $W = 60$ W, $d = 30$ cm.
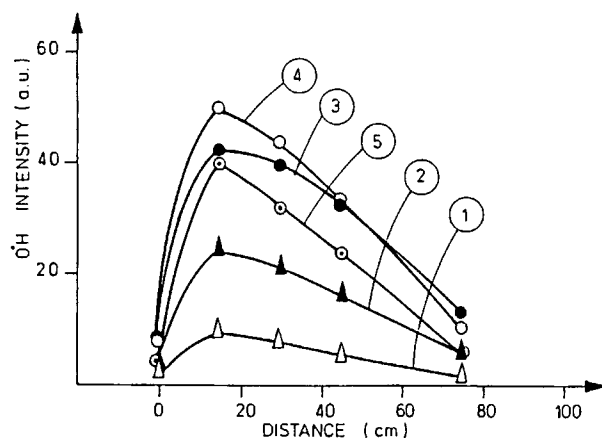
Figure 11 Effect of distance on OH intensity of H_2O plasma. (1), P = 0.065 mbar, W = 40 W; (2), P = 0.065 mbar, W = 100 W; (3), P = 0.065 mbar, W = 200 W; (4), P = 0.1 mbar, W = 200 W; (5), P = 0.2 mbar, W = 200 W.

Figure 12(b) Water contact angle vs. OH intensity. (1), PS P = 0.045 mbar, W = 60 W; (2), PS P = 0.2 mbar, W = 20 W; (3), PEI P = 0.065 mbar, W = 200 W; (4), PEI P = 0.2 mbar, d = 30 cm; (5), PEI P = 0.2 mbar, d = 15 cm.

electron energy distribution function, $\sigma_{A^* \to A}(E)$ is the cross-section for transition between the excited level of A and a lower state, and E is the electron energy.

Effect of Plasma Parameters on the OH 307.6 nm Emission Line

The intensity of the OH peak increases linearly with the electrical power (Fig. 9). The other plasma parameters influence only the slope of the curve. Both the electronic density of the plasma n_e and the mean electron's energy will be increased while power is
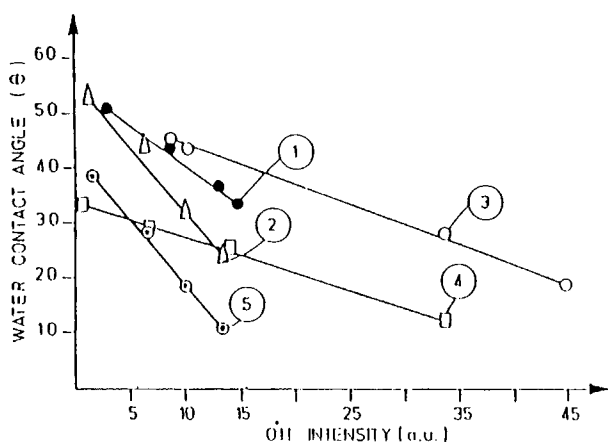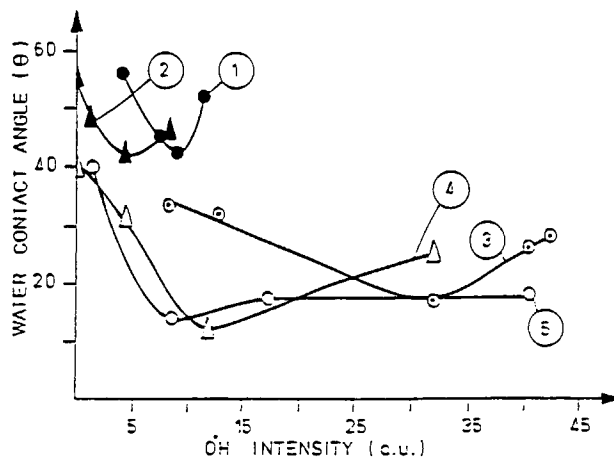
increased. According to eq. (1), an increase of I_A is expected from these two effects.

A similar dependance of I_{OH} with pressure and distance from the coil is observed (Figs. 10 and 11). The H_2O pressure giving the maximum of I_{OH} changes slightly with the other plasma parameters. In particular, the highest power (200 W) gives an I_{OH} maximum at the highest pressure. At the lowest power (20 W), no maximum is visible. Whatever the other plasma parameters, a maximum value of I_{OH} is observed at 15 cm from the coil.

Discussion

A comparison between Figures 6 and 10 (effect of pressure) and Figures 7 and 11 (effect of distance) suggests that the maximum of wettability (Θ minimum) occurs at the maximum of I_{OH}. The relation between I_{OH} and Θ has been plotted in Figures 12(a) and (b). The variation of Θ depends on two factors: (1) generation of oxygenated species in the plasma gas phase, which depends on plasma parameters (W, P, and location in the reactor); and (2) grafting probability of the oxygenated species at the surface of the polymer, which depends on the balance between etching and grafting.

In most cases [Fig. 12(a)], a linear dependance between Θ and I_{OH} is observed. It is then possible to conclude that OH radicals are responsible for the increase in wettability. In other cases [Fig. 12(b)], there is a decay of Θ followed by a stabilization or even an increase. In those cases, the mechanism leading to a decay of Θ is supposed to be more com-

Figure 12(a) Water contact angle vs. OH intensity. (1), PS P = 0.1 mbar, W = 200 W; (2), PS P = 0.1 mbar, W = 60 W; (3), PEI P = 0.65 mbar, W = 60 W; (4), PEI P = 0.1 mbar, d = 45 cm; (5), PEI P = 0.1 mbar, W = 60 W.
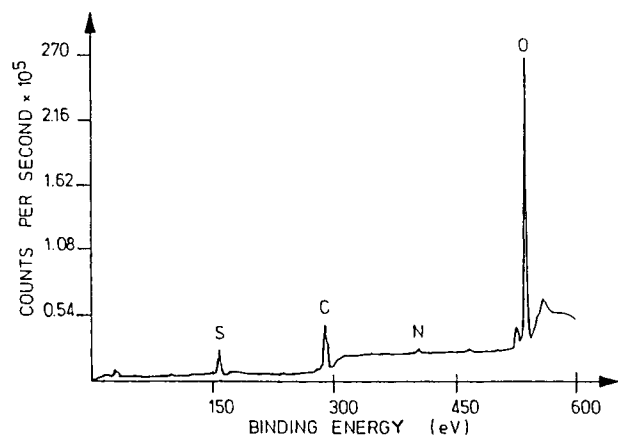
Figure 13(a) ESCA survey scan of a treated PS. *P*, 0.1 mbar, *W*, 60 W; *d*, 15 cm.
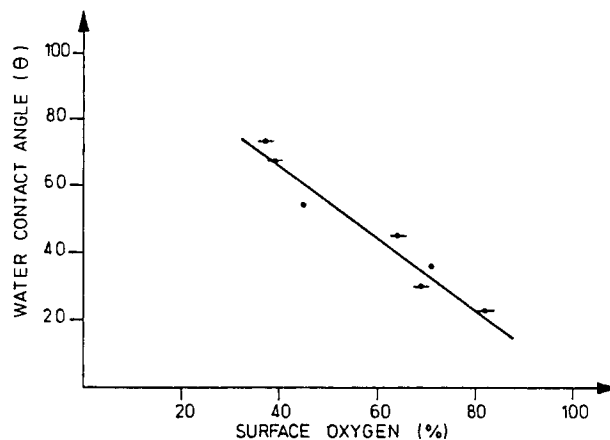

Figure 14 Water contact angle vs. surface oxygen percentage for PS membranes.

plex. A stabilization of Θ might occur in spite of the increase of the number of OH radicals because the number of acceptor sites available is limited or because the balance between etching and grafting tends to zero.

When Θ vs. I_{OH} exhibits a U-shaped curve, it means that although the number of radiative OH species increases there is a decay of oxygenated species grafted at the surfaces of samples. This could occur when plasma conditions lead to more etching than grafting. For example, as power is increased, the number of OH groups increases leading to a decay of Θ, but above a threshold power etching becomes competitive and the initial wettability of the surface can be recovered.

In the case of samples located very far from the coil or inside the coil (not reported in these figures), nonreproducible results have been found.
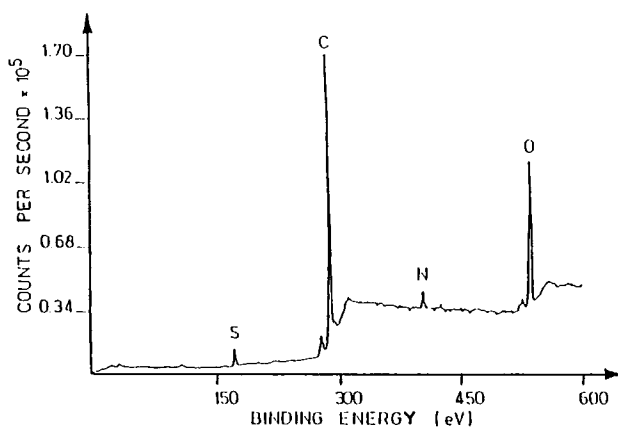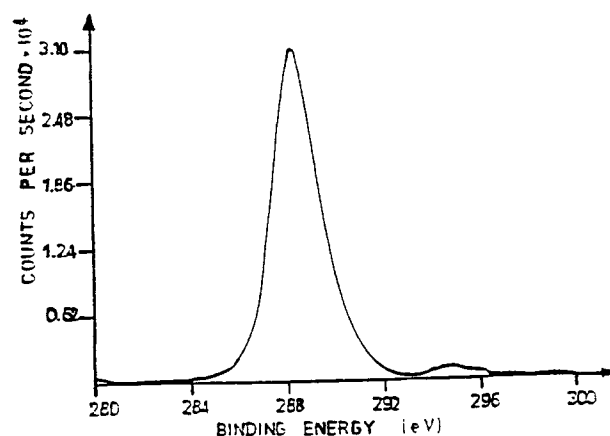

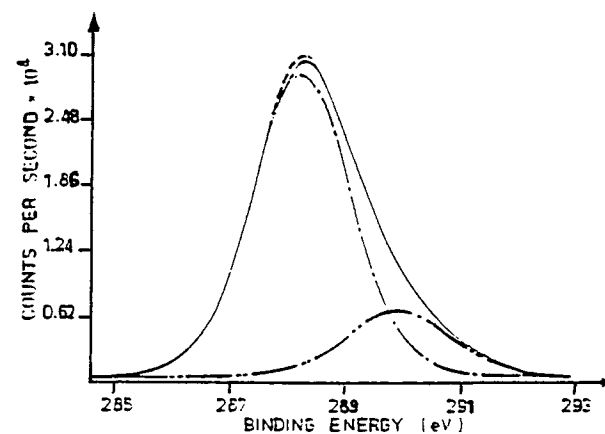

Figure 13(b) ESCA survey scan of a nontreated PS.

Figure 15(a) The C_{1s} peak deconvolution of a nontreated PS.

If etching effects are avoided or minimized, these results show that optical emission of OH radicals in an H_2O plasma is directly related to the wettability of the treated surface of the polymer.
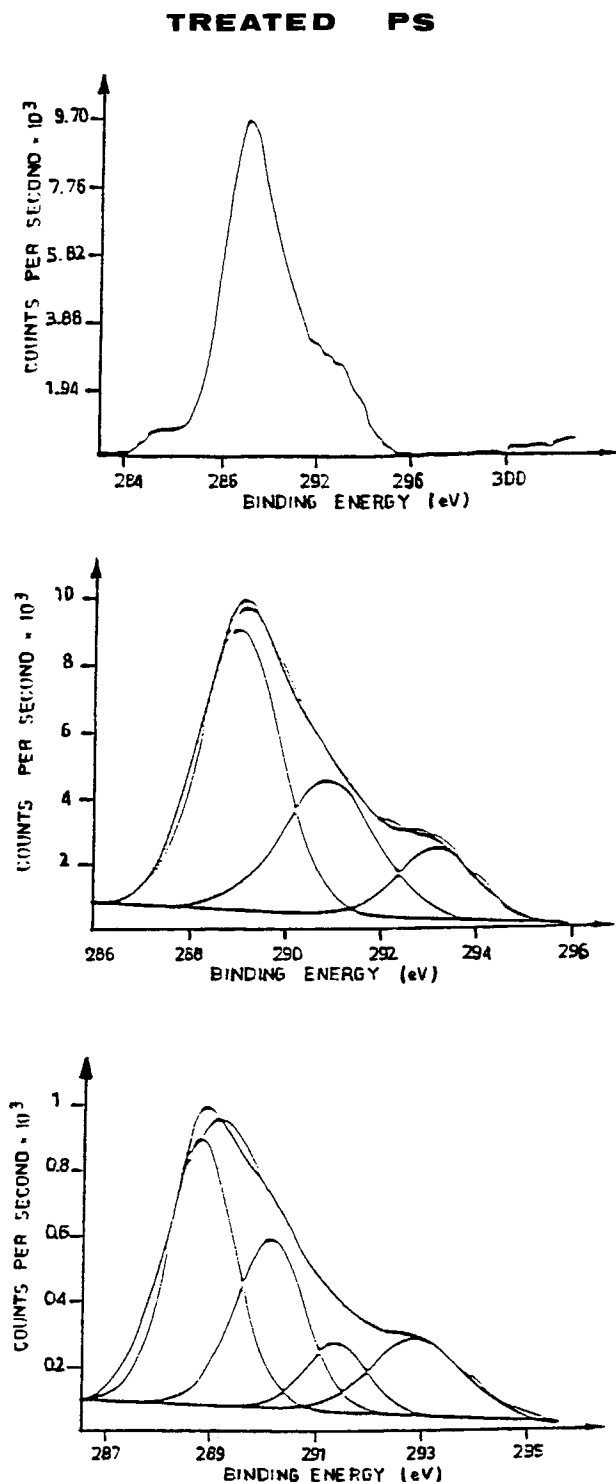
TREATED PS

Figure 15(b) The C_{1s} peak deconvolution of a treated PS. P, 0.1 mbar; W, 60 W; d, 15 cm.

ESCA Analysis of Treated Polymers

At this stage, correlation between macroscopic plasma parameters, OH emission of the plasma, and wettability of the treated surface have been established. Wettability and OH emission are supposedly related through grafting of oxygenated species at the surfaces of treated polymers. ESCA analysis is a good way to confirm this view.

In Figures 13(a) and 13(b), the survey spectra of H_2O plasma treated and nontreated PS samples, respectively, show a large increase in oxygen concentration at the surface. A stronger argument is given by Figure 14, where the contact angle is observed to decrease linearly with the oxygen content. A further understanding is provided by considering how oxygen atoms are fixed at the surface. ESCA can give some information by closer examination of the peak shape, in particular the C_{1S} peak. The deconvolution of this peak is given in Figure 15(b), while 15(a) shows the same peak for nontreated samples. Elementary peaks are listed on Tables III and IV for untreated and plasma-treated samples, respectively. As the deconvolution of the ESCA spectra is essentially a mathematical treatment of data, the deconvolved spectra may not be unique. As can be seen in Table IV, two sets of deconvolution data have been obtained from the same initial spectrum. In both cases, however, the presence of oxygen atoms involved in C—O bonds is increased for

$$
\begin{array}{c}
\text{O} \\
\text{//} \\
\text{treated samples, whereas } -\text{C} \qquad \text{groups that} \\
\text{\backslash } \quad \text{/} \\
\text{O}
\end{array}
$$

were not detected in the untreated sample now ap-

$$
\begin{array}{c}
\text{O} \\
\text{//} \\
\text{pear. The } -\text{C} \qquad \text{groups might be related to OH} \\
\text{\backslash } \\
\text{O}-
\end{array}
$$

$$
\begin{array}{cc}
\text{O} & \text{O} \\
\text{//} & \text{//} \\
\text{grafting through } -\text{C} & \text{or } -\text{C} \\
\text{\backslash } & \text{\backslash } \\
\text{O}-\text{H} & \text{O}-\text{O}-\text{H}
\end{array}
$$

functions. An energy shift between theoretical and experimental energies is observed in both cases. This is due to a well-known charging effect of the insulating surface of the samples.[14]
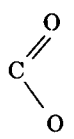
CONCLUSION

Results on plasma treatment to improve the wettability of PS and PEI membranes have been pre-

Table III   Electron Binding Engery In The Main Bonds of Untreated PS

Type of Binding	C—H and C—C	C-O	$E_{(C-O)} - E_{(C-C)}$
Energy (Theoretical)	285	286.6–286.7	1.60–1.70
Energy (Experimental)	288.27	289.93	1.66

Table IV   Electron Binding Energy In The Main Bonds of a Treated PS. P, 0.1 mbar; W, 60 w; d, 15 cm.

Type of Binding	C—H and C—C	C—O	C=O	$\begin{matrix} & O \\ & \parallel \\ & C \\ & \backslash \\ & O \end{matrix}$	$\|\Delta E_1\|$	$\|\Delta E_2\|$	$\|\Delta E_3\|$
Energy (Theoretical)	285	286.6–286.7	287.8–288.1	289.1–289.3	1.6–1.7	2.8–3.1	4.1–4.3
Energy (Experimental)	288.85	290.59	—	293.11	1.66	—	4.18
Energy (Experimental)	288.85	290.14	291.41	292.94	1.29	2.56	4.09

$$\Delta E_1 = E\begin{pmatrix} C—C \\ C—H \end{pmatrix} - E(C—O)$$

$$\Delta E_2 = E\begin{pmatrix} C—C \\ C—H \end{pmatrix} - E(C=O)$$

$$\Delta E_3 = E\begin{pmatrix} C—C \\ C—H \end{pmatrix} - E\left(\begin{matrix} & O \\ & \parallel \\ C & \\ & \backslash \\ & O \end{matrix} \right)$$

sented. The plasma has been characterised by macroscopic parameters (power, pressure, location of the sample) and also by the optical emission of the OH radical. Relationships between wettability of treated samples and the emission intensity of OH radicals have been clearly established. The effect of plasma treatment on surface composition was checked by ESCA analysis. Evidence for the relation between OH emission in the plasma and oxygen atom concentration at the surface of the treated sample has been given. From the application point of view, water drop contact angle with the surface of treated PEI and PS can be as low as 10 and 20° for PEI and PS, respectively.

REFERENCES

1. E. Marechal, *Modification Chimique des Polymères*, Laboratoire de Synthèse Macromoléculaire, Université de Paris VI.
2. J. M. E. Harper, in *Thin Films Processes*, J. L. Vossen and W. Kern, Eds., Academic Press, New York, 1978, pp. 175–204.
3. M. F. Bottin, H. P. Schreiber, J. Klemberg-Sapieha, and M. R. Wertheimer, *J. Appl. Polym. Sci., Applied Polymer Symposium* **38**, John Wiley and Sons, New York, 1984, pp. 193–200.
4. M. W. Urban and M. T. Stewart, *J. Appl. Polym. Sci.*, **39**, 265 (1990).
5. E. M. Liston, *J. Adhesion*, **30**, 199 (1989).
6. W. C. Hamilton, *J. Coll. Interf. Sci.*, **10**, 219 (1972).
7. H. Yasuda and T. Hsu, *J. Appl. Polym. Sci.*, **20**, 1769 (1976).
8. G. Mozzo, *Bulletin de la Société Chimique de France*, Colloque Adhésion et Physico-Chimie des Surfaces Solides, Mulhouse 8–10 Octobre 1969, Numéro Spécial, 1970, pp. 3219–3226.
9. L. Lavielle, *Ann. Phys. Fr.*, **14**, 1–48 (1989).
10. E. H. Adem, S. J. Bean, and C. M. Demanet, *XPS as a Tool for the Investigation of Polymers Irradiated by Energetic Ions*, VG Scientific Limited, West Sussex, England.
11. R. W. Dreyfus, J. M. Jasinski, R. E. Walkup, and G. E. Selwyn, *Pure Appl. Chem.*, **57**, 1265 (1985).
12. H. Yasuda, *Plasma Polymerization*, Academic Press, New York, 1985, Chap. 7.
13. F. Cramarossa, G. Ferraro, and E. Molinari, *J. Spectr. Radiat. Transf.*, **14**, 419 (1974).
14. M. Dessolin, L'Actualité Chimique, *Janvier*, **16** (1976).